
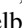




Nonequilibrium brain dynamics as a signature of consciousness

Yonatan Sanz Perl ^{1,2,3} Hernán Bocaccio ² Carla Pallavicini,² Ignacio Pérez-Ipiña,² Steven Laureys,⁴ Helmut Laufs ⁵,
Morten Kringelbach ⁶ Gustavo Deco,³ and Enzo Tagliazucchi^{2,7}

¹*Universidad de San Andrés, Buenos Aires, B1644BID, Argentina*

²*Physics Department, University of Buenos Aires, and Buenos Aires Physics Institute, Buenos Aires 1428, Argentina*

³*Center for Brain and Cognition, Computational Neuroscience Group, Universitat Pompeu Fabra, Barcelona 08002, Spain*

⁴*Coma Science Group, GIGA Consciousness, University of Liège, 4000 Liège, Belgium*

⁵*Department of Neurology, Christian Albrechts University Kiel, 24118 Kiel, Germany*

⁶*Department of Psychiatry, University of Oxford, Oxford OX12JD, United Kingdom*

⁷*Latin American Brain Health Institute (BrainLat), Universidad Adolfo Ibañez, Santiago 7910000, Chile*



(Received 18 January 2021; revised 18 May 2021; accepted 29 June 2021; published 28 July 2021)

The cognitive functions of human and nonhuman primates rely on the dynamic interplay of distributed neural assemblies. As such, it seems unlikely that cognition can be supported by macroscopic brain dynamics at the proximity of equilibrium. We confirmed this hypothesis by investigating electrocorticography data from non-human primates undergoing different states of unconsciousness (sleep, and anesthesia with propofol, ketamine, and ketamine plus medetomidine), and functional magnetic resonance imaging data from humans, both during deep sleep and under propofol anesthesia. Systematically, all states of reduced consciousness unfolded at higher proximity to equilibrium compared to conscious wakefulness, as demonstrated by the computation of entropy production and the curl of probability flux in phase space. Our results establish nonequilibrium macroscopic brain dynamics as a robust signature of consciousness, opening the way for the characterization of cognition and awareness using tools from statistical mechanics.

DOI: [10.1103/PhysRevE.104.014411](https://doi.org/10.1103/PhysRevE.104.014411)

I. INTRODUCTION

One of the defining features of living matter is the scale-dependent violation of thermodynamic equilibrium [1]. Inanimate matter frequently displays nonequilibrium dynamics, resulting from externally applied fields. In contrast, departures from equilibrium in living matter can also arise due to endogenous causes, such as complex chains of enzymatic reactions [2] driving mesoscopic mechanical processes [3]. Another characteristic of nonequilibrium dynamics in living matter is their dependence with the spatial and temporal grain; for instance, cells and larger biological structures might appear to be at equilibrium, while being sustained by nonequilibrium processes at the molecular scale [4].

Systems at thermodynamic equilibrium obey detailed balance, i.e., there are no net probability fluxes in the configuration space of the system, indicating reversible dynamics with null entropy production rate. Since the vector field representing the probability flux in configuration space becomes purely rotational for steady nonequilibrium systems, the deviation from equilibrium can be quantified using the curl of this field [5], which quantifies the degree of local circulation of the probability flux. This notion of equilibrium exists only in reference to a certain configuration space, which might reflect, in turn, a particular choice of spatiotemporal grain.

Models of nonequilibrium brain dynamics have been extensively studied in the literature in the contexts of associative learning (i.e., Hopfield networks) and decision making,

among others [6]. The phase space of excitable systems includes the important particular case of scale-free critical behavior [7]. In general, it is agreed that neural dynamics are an intrinsically nonequilibrium phenomenon; however, this is less clear for macroscopic brain dynamics [8]. A recently proposed framework to quantify entropy production from neural data acquired at a macroscopic scale [functional magnetic resonance imaging (fMRI) recordings] showed that dynamics within a reduced two-dimensional (2D) configuration space do not obey a detailed balance, and that the extent of its violation (and thus the degree of entropy production) is task-dependent [9].

In spite of these advances, the relationship between conscious states and nonequilibrium dynamics remains to be elucidated. It seems unlikely that the dynamic nature of consciousness and cognition can be sustained by a system without strong deviations from thermodynamic equilibrium at some spatial and temporal scales. Thus, brain states associated with unconsciousness could obey detailed balance at the large scale, while simultaneously being supported by nonequilibrium homeostatic processes at the cellular scale. This possibility is consistent with the characterization of unconsciousness as a state of low entropy and complexity by means of several metrics applied to large-scale brain dynamics [10–14]. We investigated electrocorticography (ECoG) recordings acquired during different states of consciousness. Compared to fMRI, this modality is better suited for the estimation of transition probabilities in configuration space, given

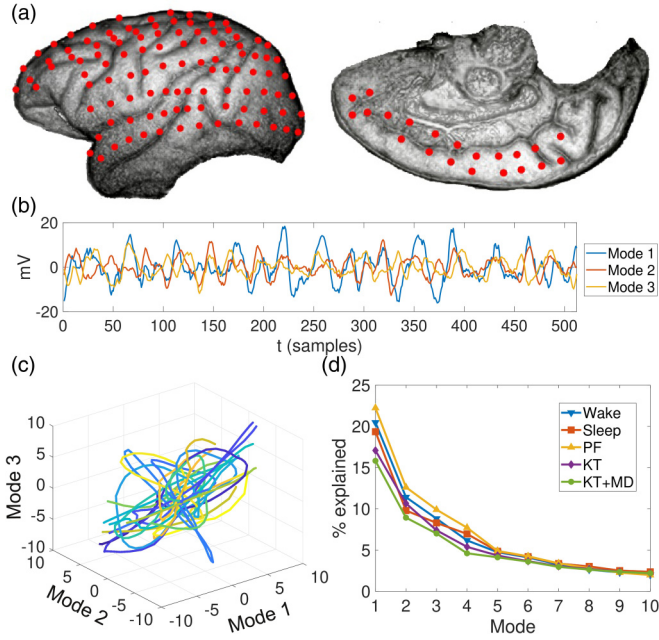


FIG. 1. Principal components of nonhuman primate ECoG signals. (a) Sample ECoG array electrode locations. (b) Temporal evolution of the three main modes of ECoG activity for an awake monkey obtained using PCA. (c) Time series of panel (b) projected on the three-dimensional configuration space (the color gradient represents the temporal evolution along the trajectory). (d) Explained variance as a function of retained principal components, plotted for all states of consciousness.

that higher temporal resolution results in better sampling of transition probabilities. We also investigated fMRI recordings by fitting semi-empirical whole-brain models to data from states of reduced consciousness, using them to produce synthetic time series with arbitrarily high temporal resolution.

II. ELECTROCORTICOGRAPHY DATA

A. Data processing and dimensionality reduction

We first considered publicly available ECoG data of nonhuman primates [128 channels from electrodes located as shown in Fig. 1(a)] during wakefulness and deep sleep (two animals, 21 sessions including eight of wakefulness), and under the effects of the following anaesthetic drugs: propofol (PF; two animals, four sessions of wakefulness, four of anaesthesia, four of recovery), ketamine (KT; two animals, four sessions of wakefulness, four of anaesthesia, four of recovery), and ketamine plus medetomidine (KT + MD; four animals, 11 sessions of wake, 11 sessions of anaesthesia, and ten sessions of recovery). All sessions were recorded with eyes closed. Time series were notch filtered to remove the power line frequency and its first harmonics (50 Hz, 100 Hz, 150 Hz) and then band-pass filtered between 1 and 500 Hz. Filtered signals were downsampled from 1 kHz to 256 Hz using linear interpolation and were standardized into z-scores prior to application of PCA. For more information on this data please see Ref. [15].

We note that experiments conducted in humans suggest that a certain degree of consciousness can be sustained during

ketamine-induced anaesthesia [16] and slow-wave sleep [17]. Given the combined difficulty of obtaining subjective reports from the animals and inferring the quality of conscious content from average brain dynamics, we assumed that their state of unresponsiveness was characterized by absent (or at least less complex) subjective experience.

Sample results obtained after dimensionality reduction are shown in Fig. 1(b) as the temporal evolution of the first three modes obtained applying PCA to ECoG of an awake animal. Figure 1(c) shows the projection of these time series on the space defined by the three principal modes, with temporal evolution represented by a color gradient from blue scales (earlier times) to yellow scales (later times). The percentage of the explained variance versus the number of components is shown in Fig. 1(d).

B. Detailed balance and entropy production

Next, we assessed the violation of detailed balance by dividing the two-dimensional space spanned by the two main modes of ECoG activity into 10×10 regular grids from -2 to 2 standard deviations from the mean [3,9]. Each recording was described as a sequence of states x_i visited over time, each corresponding to a different cell in the grid. We estimated the entropy production as a measure of equilibrium or nonequilibrium behavior by associating to each brain state a matrix P_{ij} , which contains the probability of transitioning from state x_i at time t to x_j at time $t + 1$. Finally, we calculated the entropy production as $S = \sum_{ij} P_{ij} \log\left(\frac{P_{ij}}{P_{ji}}\right)$ [9,18].

Figure 2(a) presents the average probability density (i.e., probability of visiting each cell during the recording) and the probability flux in configuration space for wakefulness, sleep, and their subtraction (wake-sleep). This flux is represented by arrows scaled according to the transition probabilities P_{ij} . Figure 2(b) (upper panel) shows that entropy production is minimal during states of reduced consciousness (sleep, KT, PF, KT + MD) compared to wakefulness. Figure 2(b) (bottom panel) shows that the curl of the probability flux was significantly reduced for all states of unconsciousness, with the exception of PF.

C. Changes in grid size

We repeated the procedure for grids with different numbers of cells, from $N = 6^2$ to $N = 20^2$ cells, and computed entropy production for each grid size. Figure 3 shows the results obtained for sleep, KT, PF, and KT + MD, as well as for the corresponding control conditions. Entropy production presented a minimum value from $N = 10^2$ to 12^2 cells and then increased monotonically. Significant differences were observed for most grid sizes.

D. Second-order transition probabilities

The calculation of entropy production by means of probability flux in configuration space assumes Markovian dynamics [18], representing a potential limitation of our analyses. To assess the potential impact of this limitation, we included a second-order term in the computation of the

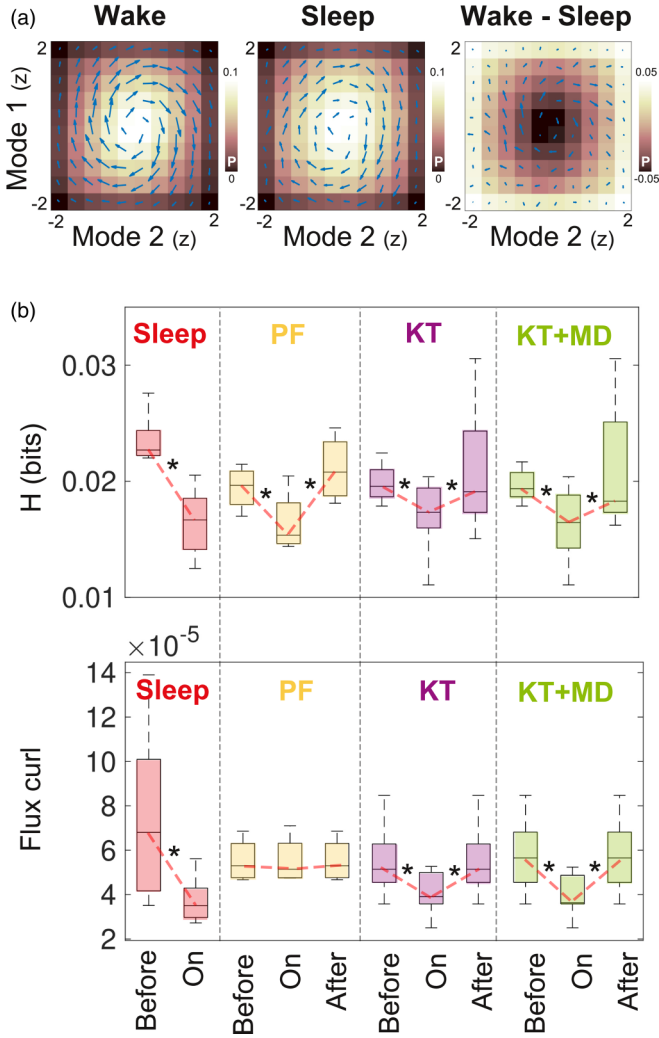


FIG. 2. Nonequilibrium entropy production is a signature of conscious states. (a) 2D configuration space defined by the two main ECoG modes (converted to z-scores) for sleep, awake, and their subtraction. Color indicates the probability of finding the state of the system within each cell in the grid. (b) Top: entropy production per state and condition. Bottom: Curl of the probability flux per state and condition. * $p < 0.05$, Wilcoxon’s test, Bonferroni corrected for multiple comparisons.

transition probabilities, i.e., $P_{i,j,k}$ [9]. The results preserved all significant differences shown in Fig. 2.

E. Entropy production versus spectral content

We compared the entropy production with the spectral power in different bands (1–5 Hz, 5–12 Hz, 12–30 Hz, 30–60 Hz), the last of these being an empirical metric that is frequently used to assess (un)consciousness [19]. Figure 4 presents scatterplots of the entropy production versus the spectral content of all experimental sessions for each condition and each frequency band (indicated by symbol type and color). We did not observe significant correlations that could be interpreted as redundant information between the spectral content and entropy production (all correlation coefficients

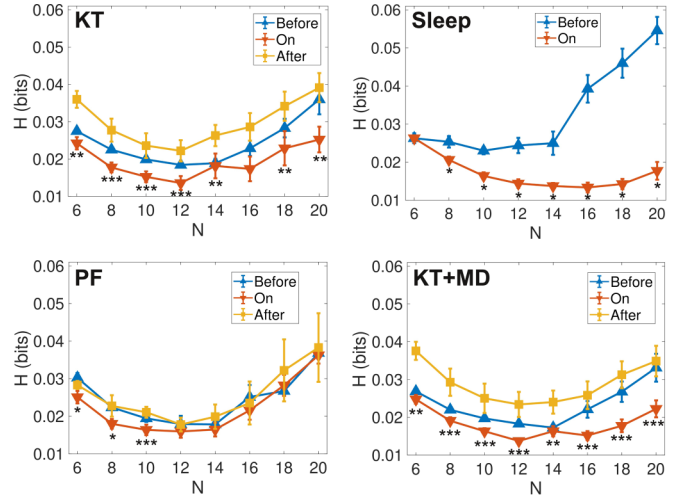


FIG. 3. Entropy production for different grid sizes. Each panel presents entropy production as a function of the square root of the number of cells for a given condition (sleep, PF, KT, KT + MD). * $p < 0.05$ before vs. on, ** $p < 0.05$ after vs. on, *** $p < 0.05$ after and before vs. on, Wilcoxon’s test, Bonferroni corrected for multiple comparisons.

and the associated p values are included in the Supplementary Material [20]).

III. MAGNETIC RESONANCE IMAGING DATA

A. Model-based data augmentation

For the purpose of fMRI data augmentation, we implemented computational models linking together multiple sources of empirical data by means of coupled local

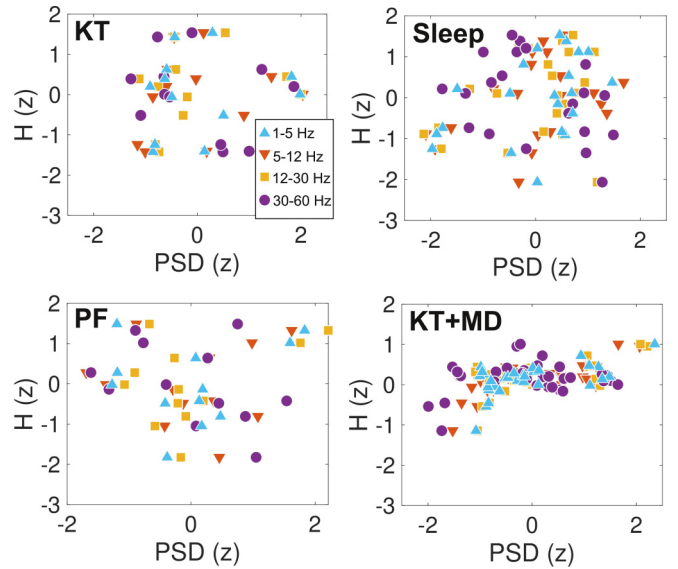


FIG. 4. Comparison between entropy production and spectral content of all sessions and conditions for frequency bands 1–5 Hz, 5–12 Hz, 12–30 Hz, 30–60 Hz, indicated with different symbol shapes and colours (both standardized to z-scores by subtracting the mean and dividing by the standard deviation). No significant correlations between these variables were found.

dynamics with different qualitative behaviors [21]. Our model incorporates empirical estimates of the large-scale structural connectivity of the brain obtained using diffusion tensor imaging (DTI), a noninvasive methodology to estimate axon bundles from water diffusion anisotropies. We computed an observable based on the large-scale functional connectivity of the brain, i.e., the linear correlation between all pairs of fMRI time series extracted from 90 predefined regions of interest spanning the whole cortical and subcortical gray matter (correlation matrix) [22]. Finally, we constructed models with heterogeneous local parameters whose variation is constrained by anatomical priors that represent boundaries between brain regions associated with specific functional systems [resting state networks (RSN)]. These RSN-specific parameters were optimized to maximize the similarity between the empirical and the simulated correlation matrices [23].

We outline this model in Fig. 5(a) (for further details see the Supplementary Information [20]). Local dynamics present dynamical criticality when the regional parameter a undergoes a bifurcation from stable fixed point dynamics ($a < 0$) to oscillatory behavior ($a > 0$) according to a Hopf bifurcation; these dynamics are coupled by the structural connectivity network inferred from DTI data, and scaled by a global coupling parameter (G). As shown in Ref. [23] this scaling factor G and the local bifurcation parameters corresponding to each anatomical prior (i.e., a value for each RSN) can be optimized to reproduce the functional connectivity measured during different states of consciousness.

B. Entropy production

We applied this optimization procedure to reproduce the empirical observables for wakefulness, for all human nonrapid eye movement (NREM) sleep stages (N1, N2, N3), and for propofol-induced sedation and loss of consciousness. We then used the optimal parameters to enhance the BOLD signal lengths of each subject ($n = 15$) up to 30 000 samples for each region of interest [24], allowing us to estimate entropy production as done with the ECoG data (Fig. 2). Figure 5(a) (bottom) presents the three main modes extracted from the simulated BOLD time series using PCA for parameters corresponding to wakefulness. Figure 5(b) presents entropy production and curl of probability flux estimated from the time series corresponding to all sleep stages and depths of propofol sedation. We found that N2 and N3 sleep (the deepest stages of NREM sleep) presented dynamics significantly closer to detailed balance than conscious wakefulness; we found the same for propofol sedation and loss of consciousness, but not for early (N1) sleep.

IV. CONCLUSION

Most of the leading theories agree that consciousness and cognition emerge from the coordinated and dynamic interplay of distributed brain activity. For example, the global workspace theory posits that consciousness is equivalent to the nonlinear and flexible percolation of sensory information throughout an anatomical connectivity backbone [25]. The dynamic core hypothesis by Edelman and Tononi identifies

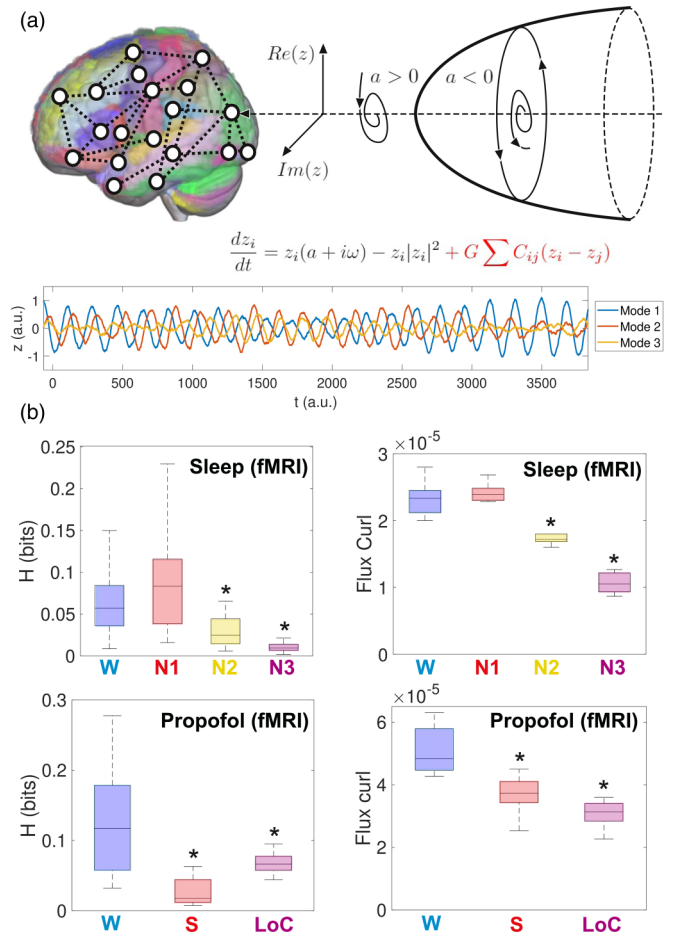


FIG. 5. Model-based fMRI data enhancement to assess nonequilibrium dynamics in the human brain. (a) Top: A whole-brain semi-empirical model presenting dynamical criticality (local Hopf bifurcation) fitted to the empirical functional connectivity of different sleep stages, using structural connectivity (DTI) to couple the local dynamics, and different RSN as priors to constraint the independent variation of local bifurcation parameters. Bottom: The temporal evolution of the three principal modes obtained using PCA over the simulated time series. (b) Entropy production (left) and flux curl (right) computed from the model fitted to empirical fMRI data obtained during wakefulness and three progressively deeper stages of human sleep (top), as well as wakefulness and two levels of propofol-induced loss of consciousness (bottom). * $p < 0.05$, Wilcoxon's test, Bonferroni corrected for multiple comparisons.

consciousness with an integrated dynamic process capable of achieving an enormous number of configurations [26]. How does the neural collective self-organize to fulfill the dynamic requirements of these theories? Our work shows that nonequilibrium brain dynamics is a general feature of conscious states. In turn, this type of dynamics can be achieved through different mechanisms, such as statistical [27–29] and dynamic criticality [30]. We note that the notion of consciousness as a unidimensional construct has been criticized [31]. We propose that our characterization captures the general complexity of ongoing conscious content, as could be operationalized, for instance, by objective analysis of verbal reports upon awakening.

Importantly, we established the independence between nonequilibrium entropy production and spectral features that are frequently used to characterize unconscious states. This observation is relevant since some of the general anaesthetic we investigated (e.g., ketamine [32]) fail to induce the type of low frequency and complexity oscillations that are indicative of reduced consciousness, suggesting that our metrics could be more general. However, these differences in spectral content could also be consistent with the presence of ongoing conscious mentation [16], a possibility that should be evaluated by applying our developments to experiments in humans.

In summary, we demonstrated a link between a very general property of the brain as a macroscopic physical system and the emergence of consciousness. Future studies should refine our conclusions, attempting to converge towards the relationship between dynamics and computation in neural tissue, one of the most challenging and long-standing problems in the field.

ACKNOWLEDGMENT

The authors acknowledge funding from Agencia Nacional De Promoción Científica Y Tecnológica (Argentina), Grant No. PICT-2018-03103.

- [1] F. Gnesotto, F. Mura, J. Gladrow, and C. P. Broedersz, Broken detailed balance and non-equilibrium dynamics in living systems: a review, *Rep. Prog. Phys.* **81**, 066601 (2018).
- [2] X. Fang, K. Kruse, T. Lu, and J. Wang, Nonequilibrium physics in biology, *Rev. Mod. Phys.* **91**, 045004 (2019).
- [3] C. Battle, C. P. Broedersz, N. Fakhri, V. F. Geyer, J. Howard, C. F. Schmidt, and F. C. MacKintosh, Broken detailed balance at mesoscopic scales in active biological systems, *Science* **352**, 604 (2016).
- [4] D. A. Egolf, Equilibrium regained: from nonequilibrium chaos to statistical mechanics, *Science* **287**, 101 (2000).
- [5] J. Wang, Landscape and flux theory of non-equilibrium dynamical systems with application to biology, *Adv. Phys.* **64**, 1 (2015).
- [6] H. Yan, L. Zhao, L. Hu, X. Wang, E. Wang, and J. Wang, Nonequilibrium landscape theory of neural networks, *Proc. Natl. Acad. Sci.* **110**, E4185 (2013).
- [7] S. de Franciscis, J. J. Torres, and J. Marro, Unstable dynamics, nonequilibrium phases, and criticality in networked excitable media, *Phys. Rev. E* **82**, 041105 (2010).
- [8] M. Esposito, Stochastic thermodynamics under coarse graining, *Phys. Rev. E* **85**, 041125 (2012).
- [9] C. W. Lynn, E. J. Cornblath, L. Papadopoulos, M. A. Bertolero, and D. S. Bassett, Non-equilibrium dynamics and entropy production in the human brain, [arXiv:2005.02526](https://arxiv.org/abs/2005.02526).
- [10] A. G. Casali, O. Gosseries, M. Rosanova, M. Boly, S. Sarasso, K. R. Casali, S. Casarotto, M.-A. Bruno, S. Laureys, G. Tononi *et al.*, A theoretically based index of consciousness independent of sensory processing and behavior, *Sci. Transl. Med.* **5**, 198ra105 (2013).
- [11] J.-R. King, J. D. Sitt, F. Faugeras, B. Rohaut, I. El Karoui, L. Cohen, L. Naccache, and S. Dehaene, Information sharing in the brain indexes consciousness in noncommunicative patients, *Curr. Biol.* **23**, 1914 (2013).
- [12] D. Mateos, R. G. Erra, R. Wennberg, and J. P. Velazquez, Measures of entropy and complexity in altered states of consciousness, *Cognitive Neurodynamics* **12**, 73 (2018).
- [13] M. Schartner, A. Seth, Q. Noirhomme, M. Boly, M.-A. Bruno, S. Laureys, and A. Barrett, Complexity of multi-dimensional spontaneous eeg decreases during propofol induced general anaesthesia, *PLoS one* **10**, e0133532 (2015).
- [14] M. Oizumi, L. Albantakis, and G. Tononi, From the phenomenology to the mechanisms of consciousness: integrated information theory 3.0, *PLoS Comput. Biol.* **10**, e1003588 (2014).
- [15] <http://neurotycho.org/>.
- [16] S. Sarasso, M. Boly, M. Napolitani, O. Gosseries, V. Charland-Verville, S. Casarotto, M. Rosanova, A. G. Casali, J.-F. Brichant, P. Boveroux *et al.*, Consciousness and complexity during unresponsiveness induced by propofol, xenon, and ketamine, *Curr. Biol.* **25**, 3099 (2015).
- [17] F. Siclari, B. Baird, L. Perogamvros, G. Bernardi, J. J. LaRocque, B. Riedner, M. Boly, B. R. Postle, and G. Tononi, The neural correlates of dreaming, *Nat. Neurosci.* **20**, 872 (2017).
- [18] É. Roldán and J. M. R. Parrondo, Estimating Dissipation From Single Stationary Trajectories, *Phys. Rev. Lett.* **105**, 150607 (2010).
- [19] C. Koch, M. Massimini, M. Boly, and G. Tononi, Neural correlates of consciousness: progress and problems, *Nat. Rev. Neurosci.* **17**, 307 (2016).
- [20] See Supplemental Material at <http://link.aps.org/supplemental/10.1103/PhysRevE.104.014411> for the correlation between entropy and spectral power; differences in spectral power between states of consciousness; entropy production computation using 3 pca; entropy production in surrogate series; the experimental procedures followed to obtain and analyze the neuroimaging data; hopf whole-brain model and comparison between empirical and simulated correlation matrices which includes Refs. [23,27,33–42].
- [21] R. Cofré, R. Herzog, P. A. Mediano, J. Piccinini, F. E. Rosas, Y. Sanz Perl, and E. Tagliazucchi, Whole-brain models to explore altered states of consciousness from the bottom up, *Brain Sci.* **10**, 626 (2020).
- [22] N. Tzourio-Mazoyer, B. Landeau, D. Papathanassiou, F. Crivello, O. Etard, N. Delcroix, B. Mazoyer, and M. Joliot, Automated anatomical labeling of activations in spm using a macroscopic anatomical parcellation of the mni mri single-subject brain, *Neuroimage* **15**, 273 (2002).
- [23] I. P. Ipiña, P. D. Kehoe, M. Kringelbach, H. Laufs, A. Ibañez, G. Deco, Y. S. Perl, and E. Tagliazucchi, Modeling regional changes in dynamic stability during sleep and wakefulness, *NeuroImage* **215**, 116833 (2020).
- [24] Y. S. Perl, H. Bocaccio, I. Pérez-Ipiña, F. Zamberlán, J. Piccinini, H. Laufs, M. Kringelbach, G. Deco, and E. Tagliazucchi, Generative Embeddings Of Brain Collective Dynamics Using Variational Autoencoders, *Phys. Rev. Lett.* **125**, 238101 (2020).

- [25] G. A. Mashour, P. Roelfsema, J.-P. Changeux, and S. Dehaene, Conscious processing and the global neuronal workspace hypothesis, *Neuron* **105**, 776 (2020).
- [26] G. Tononi and G. M. Edelman, Consciousness and complexity, *Science* **282**, 1846 (1998).
- [27] E. Tagliazucchi, D. R. Chialvo, M. Siniatchkin, E. Amico, J.-F. Brichant, V. Bonhomme, Q. Noirhomme, H. Laufs, and S. Laureys, Large-scale signatures of unconsciousness are consistent with a departure from critical dynamics, *J. R. Soc., Interface* **13**, 20151027 (2016).
- [28] A. G. Hudetz, C. J. Humphries, and J. R. Binder, Spin-glass model predicts metastable brain states that diminish in anesthesia, *Front. Syst. Neurosci.* **8**, 234 (2014).
- [29] J. R. Riehl, B. J. Palanca, and S. Ching, High-energy brain dynamics during anesthesia-induced unconsciousness, *Network Neuroscience* **1**, 431 (2017).
- [30] G. Solovey, L. M. Alonso, T. Yanagawa, N. Fujii, M. O. Magnasco, G. A. Cecchi, and A. Proekt, Loss of consciousness is associated with stabilization of cortical activity, *J. Neurosci.* **35**, 10866 (2015).
- [31] T. Bayne, J. Hohwy, and A. M. Owen, Are there levels of consciousness? *Trends Cognit. Sci.* **20**, 405 (2016).
- [32] A. Maksimow, M. Särkelä, J. Långsjö, E. Salmi, K. Kaisti, A. Yli-Hankala, S. Hinkka-Yli-Salomäki, H. Scheinin, and S. Jääskeläinen, Increase in high frequency eeg activity explains the poor performance of eeg spectral entropy monitor during s-ketamine anesthesia, *Clin. Neurophysiol.* **117**, 1660 (2006).
- [33] R. B. Berry, R. Brooks, C. E. Gamaldo, S. M. Harding, C. Marcus, B. V. Vaughn *et al.*, *The AASM Manual for the Scoring of Sleep and Associated events, Rules, Terminology and Technical Specifications* (American Academy of Sleep Medicine, Darien, Illinois, 2012), Vol. 176.
- [34] E. Tagliazucchi and H. Laufs, Decoding wakefulness levels from typical fmri resting-state data reveals reliable drifts between wakefulness and sleep, *Neuron* **82**, 695 (2014).
- [35] R. MacLaren, J. M. Plamondon, K. B. Ramsay, G. M. Rucker, W. D. Patrick, and R. I. Hall, A prospective evaluation of empiric versus protocol-based sedation and analgesia, *Pharmacotherapy: The Journal of Human Pharmacology and Drug Therapy* **20**, 662 (2000).
- [36] M. Jenkinson, P. Bannister, M. Brady, and S. Smith, Improved optimization for the robust and accurate linear registration and motion correction of brain images, *NeuroImage* **17**, 825 (2002).
- [37] T. E. Behrens, H. J. Berg, S. Jbabdi, M. F. Rushworth, and M. W. Woolrich, Probabilistic diffusion tractography with multiple fibre orientations: What can we gain? *NeuroImage* **34**, 144 (2007).
- [38] B. M. Jobst, R. Hindriks, H. Laufs, E. Tagliazucchi, G. Hahn, A. Ponce-Alvarez, A. B. Stevner, M. L. Kringelbach, and G. Deco, Increased stability and breakdown of brain effective connectivity during slow-wave sleep: mechanistic insights from whole-brain computational modelling, *Sci. Rep.* **7**, 4634 (2017).
- [39] G. Deco, M. L. Kringelbach, V. K. Jirsa, and P. Ritter, The dynamics of resting fluctuations in the brain: metastability and its dynamical cortical core, *Sci. Rep.* **7**, 3095 (2017).
- [40] Z. Wang, A. C. Bovik, H. R. Sheikh, and E. P. Simoncelli, Image quality assessment: from error visibility to structural similarity, *IEEE Transactions on Image Processing* **13**, 600 (2004).
- [41] C. Reveley, A. K. Seth, C. Pierpaoli, A. C. Silva, D. Yu, R. C. Saunders, D. A. Leopold, and Q. Y. Frank, Superficial white matter fiber systems impede detection of long-range cortical connections in diffusion mr tractography, *Proc. Natl. Acad. Sci.* **112**, E2820 (2015).
- [42] A. Messé, D. Rudrauf, H. Benali, and G. Marrelec, Relating structure and function in the human brain: Relative contributions of anatomy, stationary dynamics, and non-stationarities, *PLoS Comput. Biol.* **10**, e1003530 (2014).